Solar Array at Very High Temperatures: Ground Tests

Boris Vayner

Ohio Aerospace Institute, Cleveland, OH 44142, USA E-mail: Boris.V.Vayner@nasa.gov

ABSTRACT

Solar array design for any spacecraft is determined by the orbit parameters. For example, operational voltage for spacecraft in Low Earth Orbit (LEO) is limited by significant differential charging due to interactions with low temperature plasma. In order to avoid arcing in LEO, solar array is designed to generate electrical power at comparatively low voltages (below 100 V) or to operate at higher voltages with encapsulated of all suspected discharge locations. In Geosynchronous Orbit (GEO) differential charging is caused by energetic electrons that produce differential potential between coverglass and conductive spacecraft body in a kilovolt range. In such a case, weakly conductive layer over coverglass (ITO) is one of possible measures to eliminate dangerous discharges on array surface. Temperature variations for solar arrays in both orbits are measured and documented within the range of -150 ^{0}C +110^0 C. This wide interval of operational temperatures is regularly reproduced in ground tests with radiative heating and cooling inside shroud with flowing liquid nitrogen. The requirements to solar array design and tests turn out to be more complicated when planned trajectory crosses these two orbits and goes closer to Sun. Conductive layer over coverglass causes sharp increase in parasitic current collected from LEO plasma, high temperature may cause cracks in encapsulating material (RTV), radiative heating of coupon in vacuum chamber becomes practically impossible above 150^0 C, conductivities of glass and adhesive go up with temperature that decrease array efficiency, and mechanical stresses grow up to critical magnitudes. A few test arrangements and respective results are presented in current paper. Coupons were tested against arcing in simulated LEO and GEO environments under elevated temperatures up to 200^0 C. The dependence of leakage current on temperature was measured, and electrostatic cleanness was verified for coupons with antireflection (AR) coating over ITO layer.

1. ENCAPSULATED COUPON

Plasma parameters around coupon in simulated LEO environment were obtained by sweeping four Langmuir probes (three spherical probes with 1.9 cm diameter each, and one flat probe with 1 cm diameter). Electron beam current density (simulated GEO environment) was measured with Faraday cap, and surface potential was measured and recorded by scanning coupon in horizontal direction with TREK probe. Coupon temperature was measured and recorded by five thermocouples (T-type) mounted on the back side. Video camera and VCR were used to determine arc site locations. Differential charging was

One of a few possible solutions in preventing surface discharges on solar array is encapsulation of interconnectors and gaps between strings (Fig.1).

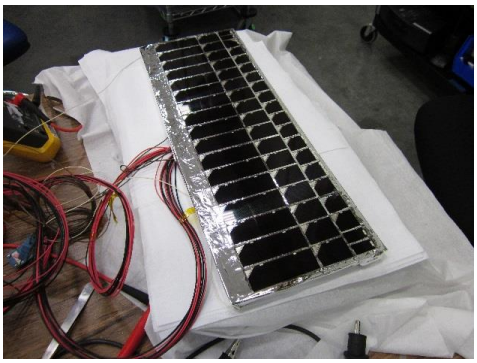

Figure 1. Test coupon with fully encapsulated all dielectric-conductor junctions.

This coupon had three strings with seventeen cells in each string, interconnectors and gaps between strings were covered with RTV, and edges were wrapped with thin conductive foil [1]. Tests were performed in horizontal vacuum chamber (Tenney) with 1.8 m diameter and 2 m length (Fig.2).

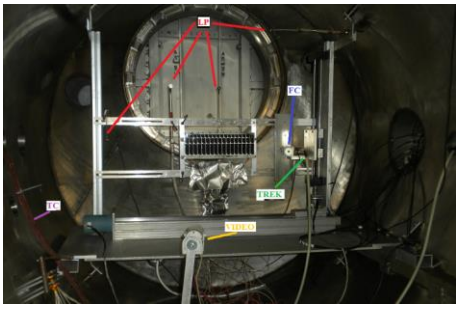

Figure 2. Coupon and diagnostic equipment are shown inside vacuum chamber.

created by biasing all strings with high-voltage power supply through *RC* circuit (R=10 kΩ, C=0.22 μF for LEO simulations, and R=1 MΩ and C=50 nF for GEO simulations). Arc current and voltage pulse wave forms were registered by respective probes and four channel oscilloscope (Fig.3). The detailed test procedures and appropriate equipment are described in Ref. 2.

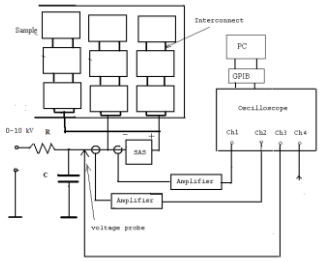

Figure 3. Circuitry diagram for registering primary ESDs and sustained arcs

The results of tests against primary arc inception in simulated LEO environment are summarized in Table 1. Tests were performed in Xenon plasma with electron number density of N_e=10^6 cm^{-3} and electron temperature of T_e=0.2 eV.

Thus, arc inception voltage was found to be around 300 V that exceeded array operational voltage more than four times. Current collection was measured in microamperes range, and it was concluded that LEO environment would be benign in sense of current collection and arc inception.

This coupon had anti-reflection (AR) coating over coverglass and no ITO layer; therefore, differential charging was expected in simulated GEO environment. Heating coupon to high temperatures might (or might not) cause the contamination of chamber volume with undesirable gases. In order to monitor this possible impurity a quadrupole mass spectrometer (RGA) was used during the test.

Table 1. Primary arc inception in simulated LEO environment.

No	:Bias: (V)	Temperature: ºC	Time: (min)	Numb. of arcs:
1.	**120**	**176**	**30**	**0**
2.	**160**	**176**	**30**	**0**
3.	**200**	**178**	**30**	**0**
4.	**240**	**177**	**30**	**0**
5.	**280**	**179**	**30**	**0**
6.	**320**	**180**	**30**	**0**
7.	**280**	**148**	**30**	**0**
8.	**320**	**148**	**30**	**2**
9.	**160**	**9**	**30**	**0**
10.	**200**	**9**	**30**	**0**
11.	**240**	**10**	**30**	**0**
12.	**280**	**11**	**30**	**0**
13.	**320**	**11**	**30**	**2**

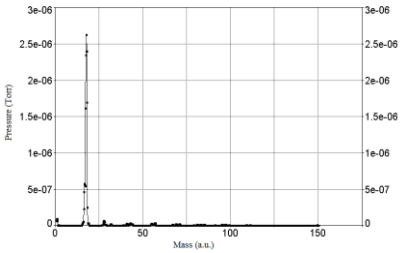

a)

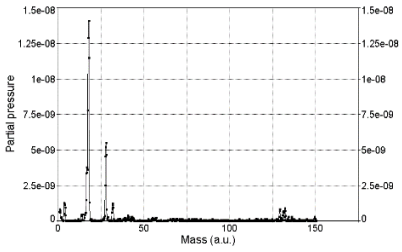

b)

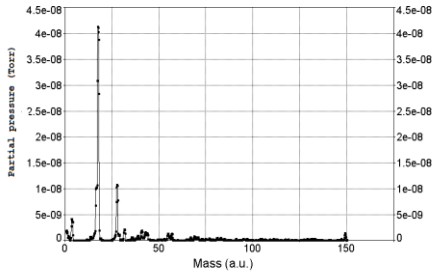

c)

Figure 4. Partial pressures of residual gases are shown: a) initial at 9^0 C; b) after few days of pumping down at 15^0 C; c) the end of test at 175^0 C.

It is seen in Fig.4 that pumping down for a few days resulted in significant decrease in water vapor partial pressure – from 2.7 μTorr to 0.013 μTorr, while heating sample from 15^0 C to 175^0 C caused minor rise in vapor pressure up to 0.04 μTorr. No other contaminating species were found at the partial pressure level above 5 nTorr. Sample was biased -4 kV, and TREK scan was performed in horizontal direction along three strings. One example of recorded potential is shown in Fig.5.

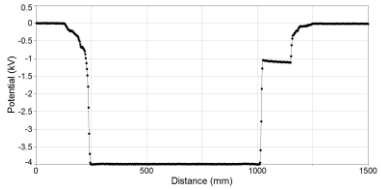

Figure 5. Surface potential is shown for biased sample before irradiation

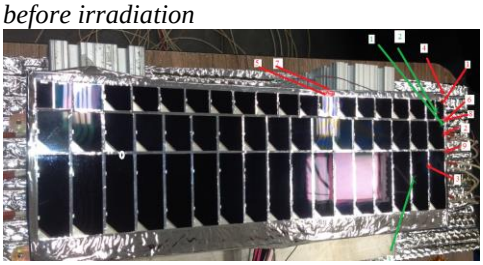

Figure 7. Arc sites are shown for test at 175 C (red), and for test at 9 C (green).

Arc current and voltage pulse wave forms had not revealed any peculiarities, and they resembled multiple wave forms observed for discharges on different samples at ambient temperature (Fig.8). Then coupon was irradiated for 20 minutes with electron beam of 4.8 keV energy and 6 nA/cm^2 current density. Obtained differential charging reached 600-700 V (Fig.6).

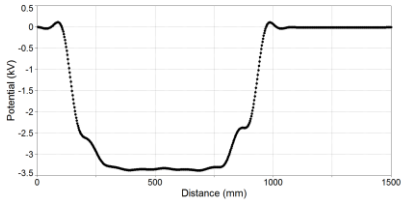

Figure 6. Surface potential is shown after 20 minutes irradiation with electron beam.

Three arcs were registered during irradiation of coupon at 9^0 C, and nine arcs were recorded at elevated coupon temperature of 175^0 C (Fig.7).

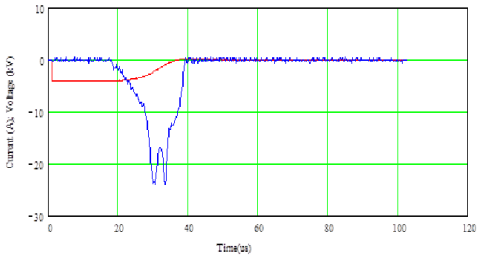

Figure 8. One example of discharge initiated at coupon temperature of 175^0 C.

Three arcs were located in the gaps between strings. Visual inspection did not reveal any flaws in RTV coating but it might mean that microscopic search should be performed – and it was not done at the time. All other arcs were located on the edge of the foil (Fig. 7), and it was someway surprising because one could not expect formation a triple junction with inverted potential gradient near foil edges. In order to understand physical mechanism of arc inception three different ways of foil biasing were investigated: 1) foil

was grounded through 1.5 MΩ resistor; 2) foil was biasing together with strings through 1.5 MΩ resistor; and 3) foil was connected to strings with one wire (Fig. 9).

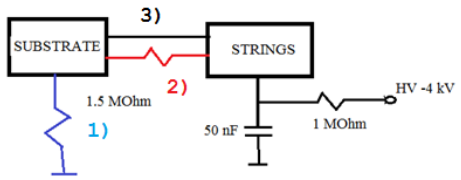

Figure 9. Three different circuitry diagrams that were used in GEO arcing tests.

The results were the following:

1. Grounded substrate-NO ARCS at all.
2. Substrate connected to strings through 1.5 MΩ resistor: 8 arcs for 46 minutes at 8° C; 8 arcs for 4 minutes at 160° C.
3. Substrate connected to strings: 3 arcs for 30 minutes at 8° C; 9 arcs for 5 minutes at 160° C.

All results of testing in simulated GEO environment are summed up in Table 2.

Table 2. The Results of GEO Testing

No.:	Bias kV	:Beam Energy: keV	Curr. Dens: nA/cm^2	Temperature: °C	Diff.Voltage: V	No. of arcs:	:Remarks:
1.	**4**	**4.8**	**9**	**6**	**500**	**0**	
2.	**4.5**	**5.3**	**6.7**	**8**	**700**	**0**	
3.	**4.5**	**5.3**	**10**	**8**	**800**	**3**	
4.	**4**	**4.8**	**6**	**176**		**9**	**for 5 minutes**
5.	**4**	**4.8**	**3.5**	**38**		**0 for 30 min.**	**Grnd.Substrat**
6.	**4**	**4.8**	**10**	**8**		**8 for 46 min.**	**Subst.to cells With R=1.5MΩ**
7.	**4**	**4.8**	**10**	**9**		**0 for 30 min.**	**Grnd.Substr.**
8.	**4**	**4.8**	**10**	**153**		**0 for 30 min**	**Subst.grnd. With R=1.5MΩ**
9.	**4**	**4.8**	**10**	**160**		**8 for 5 min**	**Substr.to cells With R=1.5MΩ**
10.	**4**	**4.8**	**10**	**160**		**4 for 14 min**	**Subst.to cells**

Arc rate for conventionally designed coupon should demonstrate quite opposite dependence of arc rate on temperature [3,4]. Kapton tape (or its adhesive) may play role in the reversed dependence observed. Moreover, in second case foil cannot be considered as vacuum arc cathode because resistor would diminish arc current significantly. Only one visible trace of arcing was found on right side of the coupon (Fig.10). It is well known that the resistivity of dielectrics decreases with increasing temperature [5,6]. Leakage current was measured between strings and substrate for temperature range of 70° C – 170° C (Fig.11). Obviously, leakage current of 10-15 μA cannot influence solar array performance at elevated temperatures.

Coupon was also tested against sustained arc (SA) inception in simulated LEO environment. String 2 (middle) was biased negatively through RC circuit, and Solar Array Simulator (SAS) was installed between string 2 (negative pole) and strings 1&3 (positive pole). Test was performed at 13° C with SAS

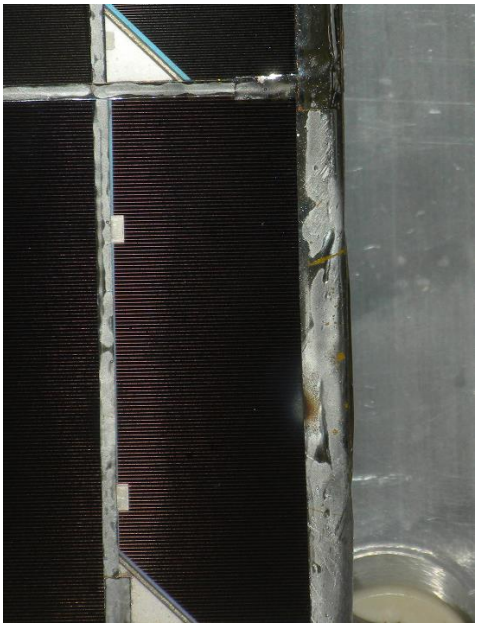

Figure 10. Visible trace of arc was found on edge of foil.

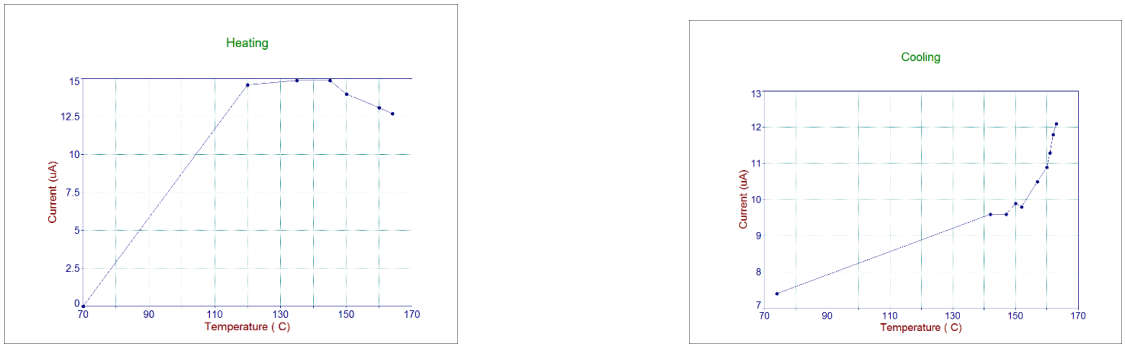

Figure 11. Voltage of 300 V was applied between strings and substrate.

voltage of 100 V and current limit of 0.1 A. No one Temporary Sustained Arc (TSA) was observed after initiating of 10 primary arcs. Then temperature was raised to 180° C and tests against SA inception were performed for the following SAS parameters: 50 V and 1.6 A (10 arcs), 50 V and 2 A (10 arcs), and 50 V and 2.4 A (20 arcs).No one indication of TSA was observed. Typical example of pulses is shown in Fig. 12.

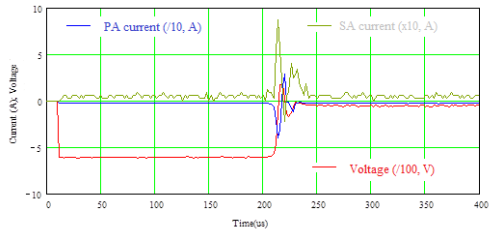

Figure12. One example of pulses for SA test: bias-600 V, PA peak -40 A, SAS current peak 0.8 A.

Dark current tests after all arcs had not revealed any damages to strings 1,2,&3. Finally, internal resistance was measured between strings and substrate with FLUKE:

At coupon temperature of 10° C the resistance was $R=\infty$, and at 160° C it was $R=0.9$ MΩ.

The results of testing against SA are shown in Table 3.

Table 3. SUSTAINED ARC TEST

No.:	Bias: V	SAS V	SAS A	:No.of PAs :	No. of SAs :	:Temp. : °C
1.	300	100	0.1	9	0	13
2.	320	50	1.6	10	0	170
	540					
3.	500	50	2	10	0	160
4.	500	50	2	10	0	180
5.	600	50	2.4	10	0	180
6.	600	50	2.4	10	0	180

2. ELECTROSTATICALLY CLEAN COUPON

For some space missions electrostatic cleanness is very important requirement [7]. Practically, it means that potential differences along spacecraft surfaces must be lower than well determined number. Solar array surface is the most crucial example of significant potential gradient-from spacecraft body potential at

the negative end to the operational voltage at the positive end of the string in LEO, and up to kilovolt potential differences in GEO. However, if all coverglasses were covered with ITO layer connected to spacecraft body, and all interconnectors and gaps between cells were covered with RTV and shielded from surrounding plasma by strips of grounded foil then (obviously) the potential gradient along the surface would be close to zero. The problem is AR coating that solar array designers refuse to abandon – it provides about 1% addition to array efficiency. AR coating (magnesium fluoride) is dielectric, and it can be charged positively by secondary electron emission. Due to very low thickness of this coating (about 100 nm) even tiny electric conductivity would not allow developing significant electric field across the AR layer but potential difference of 10-20 V seemed possible in GEO. The purpose of test described below was to determine residual potential of comparatively large coupon in simulated GEO environment. Test coupon contained seven strings with fifteen cells in each string rigidly mounted on aluminum frame. Coupon was mounted vertically in vacuum chamber (Tenney) at the distance of 1.2 m from two electron guns (Fig.13).

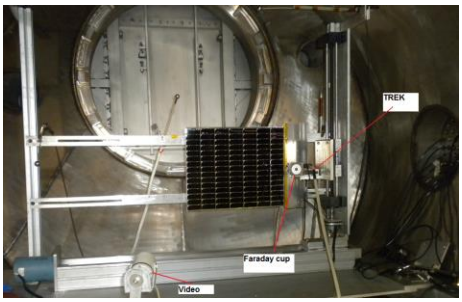

Figure 13. Coupon is shown mounted inside chamber.

The key challenge of this experiment was to measure residual potential of a few volts (if any) when average recorded potentials were equal to 3.5-4 kV. There were sources of such systematic errors as differences in power supply gauge readings and TREK recorded numbers, nonparallel probe trajectory and sample plane, and floating "zero" in TREK controller that could be determined and taken into account by multiple scans of coupon surface before irradiation and correcting "zero" point in advance of each run with grounded metal plate mounted on right side of the coupon (Fig. 13). Random errors were caused by TREK probe vibration, local deviations of coupon surface from perfect flatness, and nonhomogeneous surface charging. During the tests, all strings and titanium substrate were electrically insulated from chamber ground. Positive and negative wires of all strings were connected together and biased negatively with high-voltage power supply through RC-circuit (R=1 MΩ, C=50 nF). Substrate was connected to the same point with a separate cable. Thus, whole structure (strings, substrate, cables, TC wires, bolts, etc) had a negative potential of 3.5-4 kV with respect to the chamber walls. Such wiring simulated spacecraft body ground, and negative bias corresponded to high negative potential attained by spacecraft in GEO eclipse.

At the first stage, coupon was biased -4kV and surface potential was measured with TREK probe (Fig.14).

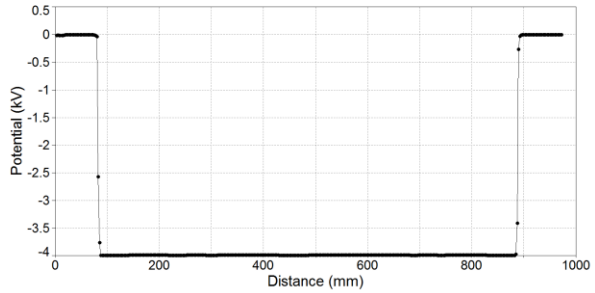

Figure 14. Potential distribution along the horizontal line in both directions (right to left and back).

Statistical analysis of numbers between points 90 mm and 890 mm resulted in coupon surface potential U=-

3.987(0.0014) kV. Thus, systematic error was about 13 V and statistical dispersion was 1.4 V. These numbers can be expressed in relative units:

$$\delta_{sys} = \frac{\Delta U_{sys}}{U} = 0.325\% \quad \text{and}$$

$$\delta_{st} = \frac{\Delta U_{st}}{U} = 0.0035\% \qquad (1)$$

At the second stage, coupon was biased -3.5 kV and irradiated with electron beam of 4.3.keV energy and 3 nA/cm^2 current density. One more scan was performed after 15 minutes of irradiation. Statistical analysis resulted in systematic error of 18 V (δ_{sys}=0.51%) and dispersion of 4.8 V (δ_{st}=0.14%) . Systematic error can be caused by: 1) differences in readings between power supply voltmeter and TREK probe; 2) residual surface charge.

Last scan was performed after 15 minutes of irradiation with beam current density of 10 nA/cm^2. The result was *U*=3.481 (0.002) kV. Thus, standard deviation was determined as 2 V across coupon. Maximum voltage was 3.487 kV and minimum voltage was 3.475 kV. These numbers allow concluding that the variations of residual differential potential did not exceed 6 V (3σ). After comparing systematic errors from the first scan (13 V, no irradiation) and from the last scan (18 V, 15 minutes irradiation) one can conclude that residual homogeneous potential did not exceed 5 V.

Last test was performed with bias voltage of -3.5 kV and beam current of 13 nA/cm^2. Coupon had been irradiated for 20 minutes, statistical characteristics of scan were the same as for previous one, and no arc on coupon surface was observed.

At the beginning of the test a few discharges were observed on edges of the coupon (Fig.15, red circles).

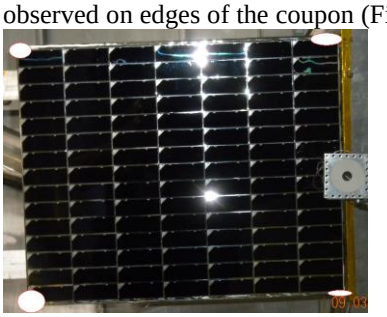

Figure 15. Arcs were observed in circled areas.

Visual examination revealed peculiar features (sharp points, gap between foil and surface) that should be fixed for further experiments. These areas were covered with Kapton tape, and no more arcs on coupon surface were observed in subsequent tests.

In order to improve the precision of measurements special setup with small coupon was implemented (Fig.16).

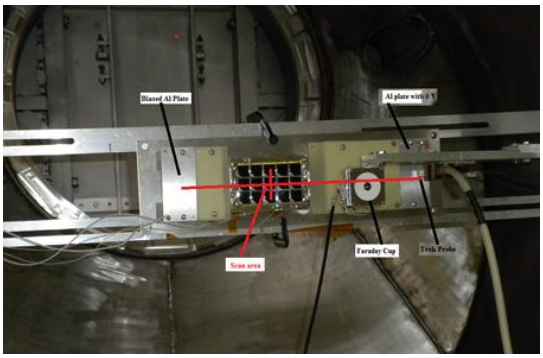

Figure 16. Setup for surface potential measurements.

Scan area was built as a flat surface consisting of (right to left) aluminum plate with zero potential, fiberglass plate (yellow), sample, fiberglass, and aluminum plate biased to the sample solar cells potential. The systematic errors caused by geometry were checked by scanning the surface at bias voltage of -3 kV with the following results: coupon, right-left: *U*=-2972 V (2.9); left-right: *U*=-2974 V (2.9); Al plate *U*=-2972 V (1.9). Thus, there was no deviation in TREK readings due to geometry. The results of seven runs are summarized in Table 4. Thus, ITO+AR layers provided practically perfect shield for internal potential. The reason for wide scattering in residual potentials (0-20 V) obtained in this test is not clear now.

No arc was observed for additional 40 minutes irradiation with 5.8 keV beam.

An estimate for residual potential can be obtained from the results of measurements: TREK scans were performed in both directions with time interval of one minute, and no difference in surface potentials was found. It means that charge relaxation time is much longer than one minute:

Table 4. Residual potentials for ITO+AR layers.

No.	:Bias : (kV) :	Beam Energy (keV):	Curr.(nA/cm^2)	: Time : (min) :	Res. Potential: (V)	Stdv : (V) :	String :
1.	3	3.8	10	20	16	6	middle
2.	5	5.8	10	20	11	7	middle
3.	5	5.8	10	30	13	8.5	upper
4.	0	-	-	-	21	3.8	upper
5.	3	3.8	10	30	1	6.2	upper
6.	3	3.8	10	30	14	6	bottom
7.	5	5.8	10	30	0	3.2	bottom

$$\tau = \frac{\varepsilon\varepsilon_0}{\sigma} >> 60s \qquad (2)$$

Dielectric permittivity of magnesium fluoride is ε=5.5, and the upper limit for conductivity can be calculated from Eq. 2:

$$\sigma_{\max} = 8 \cdot 10^{-13} S/m \quad (3)$$

This estimate (3) is very crude but it allows calculating leakage current density through AR layer with thickness *d*:

$$j_{\max} = \sigma_{\max} \cdot \frac{U}{d} \qquad (4)$$

Substituting respective magnitudes for thickness *d*=100 nm and voltage drop *U*=20 V one can obtain j_{max}=16 nA/cm^2. Thus, the suggestion of bleeding surface charge through AR layer in current experiment seems quite reasonable. There are no published data concerning AR conductivity but our measurements of this parameter performed in simulated LEO conditions resulted in practically the same number: $\sigma \approx 10^{-12}$ S/m [8]. It is worth noting that AR layer conductivity depends strongly on its chemical composition and methods of application [9] but this issue is beyond the scope of current paper.

3. CONCLUSIONS

The tests demonstrated clearly that conductive heating of solar array coupon allowed testing against differential charging at high temperatures even in comparatively small plasma chamber. Contamination of chamber volume due to outgassing was absolutely insignificant, and decrease in dielectric resistivity did not cause any substantial leakage current. RTV grouting of all gaps between strings resulted in rising arc threshold well above differential voltages expected for spacecraft in LEO. However, in order to avoid arcing in GEO coverglass should be covered with weakly conductive layer (ITO). Full encapsulation of coupon with ITO connected to substrate allowed achieving a very high electrostatic cleanness. Influence of cosmic radiation and thermal cycling on RTV properties (aging) needs additional investigations.

4. REFERENCES

1.Donegan, M., Decker, R., Raouafi, N., Lario, D., and Bernasconi, P. “Surface Charging Analyses for the Solar Probe Plus Mission”, 11th Spacecraft Charging Technology Conference, Albuquerque, NM, 2010.

2. Vayner, B., Galofaro, J., and Ferguson, D. “Interactions of High-Voltage Solar Arrays with Their Plasma Environment: Ground Tests”, *Journal of Spacecraft and Rockets*, Vol.41, No.6, 2004, pp.1042-1050.

3. Vayner, B., and Galofaro, J. “ ARCING ON SOLAR ARRAYS AT EXTREMELY LOW TEMPERATURES”, 21th SPRAT, October 5-9, 2009, Cleveland, Ohio.

4. Vayner, B., and Galofaro, J. “ARCING ON SOLAR ARRAYS AT LOW TEMPERATURES”, AIAA Paper 2010-75, Orlando, Florida, Jan. 2010.

5. Fused Silica Glass, Tosoh Corporation, Advanced Materials Division, http://www.tosoh.co.jp

6. Morgan, B. “Electrical Resistivity of DC 93-500 Silicon Adhesive”, Aerospace Report No. TR 2003 (1465)-1, 2003, 9 pp.

7. Boca, A., Blumenfeld, P., Crist, K., Flynn, G., McCarty, J., Patel, P.,Sarver, C., Sharps, P., Stall, R., Mark Stan, M., and Tourino, C. “Array-Design Considerations for The Solar Probe Plus Mission”, 37th Photovoltaic Specialist Conference, Seattle, WA, June 19-24, 2011.

8. Vayner, B., Ferguson, D., and Galofaro, J. “Quartz-Indium Tin Oxide-Magnesium Fluoride Sandwich in a Low Density Plasma”, Proceedings of the 4th World Conference on Photovoltaic Energy Conversion, Waikoloa, Hawaii, May 4-8, 2006.

9. Dever, J.A., Rutledge, S.K., Hambourger, P.D., Bruckner, E., Ferrante, R., Pal, A., Mayer, M., and Pietromica, A. “Indium Tin Oxide-Magnesium Fluoride Co-Deposited Films for Spacecraft Applications”, NASA/TM—1998-208499, 20 pp.